



Study on tool wear in longitudinal-torsional composite ultrasonic vibration–assisted drilling of Ti-6Al-4V alloy

Yingjian Tian¹ · Ping Zou¹ · Di Kang¹ · Fan Fan¹

Received: 26 November 2020 / Accepted: 2 February 2021 / Published online: 17 February 2021
© The Author(s), under exclusive licence to Springer-Verlag London Ltd. part of Springer Nature 2021

Abstract

Severe tool wear is always considered as a main negative result in the process of drilling Ti-6Al-4V alloy. Although the idea of employing one-dimensional longitudinal ultrasonic vibration in the drilling process to reduce tool wear has been proposed for many years, studies on longitudinal-torsional composite ultrasonic vibration–assisted drilling (LT-UAD) are seldom reported. LT-UAD is a hybrid machining process in which high-frequency and low-amplitude vibrations are superimposed simultaneously on the rotational direction and the axial direction of the drilling bit respectively. In this study, a hollow vibration converter with thread grooves is presented for LT-UAD purpose. Based on an in-depth kinematic analysis, a condition for separating the tool from the workpiece is derived, indicating that a lower feed rate, a lower spindle speed, and a higher amplitude are more advantageous. Machining experiments are performed, wherein good agreement is found between the experimental and theoretical results. The results show that LT-UAD has obvious advantages over longitudinal ultrasonic vibration–assisted drilling and conventional drilling in reducing tool wear. Additionally, the influences of the vibration amplitude, spindle speed, and feed rate on the flank wear width are analyzed, revealing the influences of the three factors in descending order are feed rate, amplitude, and spindle speed. The optimum machining parameters are obtained as 23 μm of amplitude, 385 r/min of spindle speed, and 0.06 mm/r of feed rate. Furthermore, a reliable regression model of flank wear width is established based on response surface methodology. With this prediction model, the flank wear width of drill bit under different machining parameters can be accurately predicted.

Keywords Ti-6Al-4V alloy · Longitudinal-torsional composite vibration · Ultrasonic vibration assisted drilling · Tool wear · Machining parameter optimization · Prediction model

1 Introduction

Due to the excellent properties such as low weight, high corrosion resistance, and high strength, Ti-6Al-4V alloy has been found widely used in aerospace industries to make airframe and engine components in recent years [1, 2]. In these fields, hole machining is always considered to be a key process because a large number of equipment holes need to be manufactured [3]. There are mainly three methods to process holes in Ti-6Al-4V alloy, namely drilling, electro discharge machining (EDM), and laser machining. However, the processing time of EDM and laser machining are much more than

that of drilling and the quality of the finished surfaces is poorer. Undoubtedly, drilling processing is an extensively used and economic method of hole machining in Ti-6Al-4V alloy when both productivity and machining quality are considered. However, in the drilling of Ti-6Al-4V alloy, excessive heat is generated at the cutting zones due to high chemical reactivity and low thermal conductivity properties [4]. As a result, drill bits are subjected to severe wear and adhesion of the chips, which causes great troubles for industries.

Many attempts have been made to reduce tool wear and achieve better hole quality in drilling of Ti-6Al-4V alloy, including the use of cutting fluid [5] and heat sink [6, 7] to reduce the temperature at the cutting zones, using good performance coated tools [8], optimizing cutting parameters [9] and tool geometry parameters [10]. However, cutting fluids have a significant negative impact on manufacturing costs, human health, and the environment. In addition, optimizing cutting parameters and tool geometry parameters is

✉ Ping Zou
pzou@mail.neu.edu.cn

¹ School of Mechanical Engineering and Automation, Northeastern University, Shenyang 110819, China

undoubtedly time-consuming and costly for the reason that a lot of experiments are necessary. Therefore, it is desirable to develop a cost-effective drilling process for Ti-6Al-4V alloy.

As a new type of mechanical processing method, ultrasonic vibration-assisted machining (UAM) offers a better alternative and solution to the challenges of cutting difficult-to-machine materials such as Ti-6Al-4V alloy [11], Ni-Alloy 718 [12, 13], and 304 austenitic stainless steel [14, 15]. Ultrasonic vibration-assisted drilling (UAD) is a kind of UAM, and the advantages of UAD in extending tool life, reducing cutting force, cutting temperature, and improving machining quality have been proven by many researchers. Zhang et al. [16] found that the drill life was increased about four times at most compared with conventional drilling (CD) methods when suitable amplitude was used. Zhang et al. [17] obtained an optimal processing condition experimentally and they indicated that the thrust and the torque by the vibration drilling method are reduced by 20–30% compared with conventional drilling. Azarhoushang and Akbari [18] conducted a comparison test between CD and UAD of Inconel 738-LC, which proved that the quality of the hole was improved by 60% by UAD. Barani et al. [19] revealed that UAD offers less built-up edge (BUE) and better surface quality compared to CD. The influence of ultrasonic amplitude and rotational speed on surface roughness and cutting force was studied by Baghlani et al. [20], interpreting that the surface quality was significantly improved and the thrust was reduced by 40% with the application of ultrasonic vibrations. Mohammad Lotfi and Saeid Amini [21] demonstrated that lower formation of BUE was produced and lower adhesion of working material on the body of drill bit was observable in UAD in contrast to CD. Wei Liang et al. [22] revealed a great reduction in thrust force, cutting heat, and tool wear by applying ultrasonic assistance in the drilling of titanium alloy. In addition, the advantages of UAD in chip breaking have also been illuminated through theory and experiments by Chen et al. [23, 24], which interpreted that thin and smooth chips were obtained when suitable cutting parameters were applied in the UAD of Inconel 718.

According to previous studies, most researches focus on analyzing the advantages of longitudinal ultrasonic vibration-assisted drilling (L-UAD), in which one-dimensional (1D) longitudinal ultrasonic vibration is superimposed on the feeding movement of a drill bit. However, literature about the longitudinal-torsional composite ultrasonic vibration-assisted drilling (LT-UAD), which allows the tool to vibrate simultaneously in the axial direction and circumferential direction, is extremely insufficient, not to mention the corresponding theoretical analysis. The direction of ultrasonic vibration application is reportedly critical [25]. Inspired by much better performance of two-dimensional (2D) vibration than that of 1D vibration in UAM [26–29], this study introduces a 2D (longitudinal and torsional directions)

vibration in UAD in order to further reduce tool wear. In previous studies, there are mainly two methods to achieve longitudinal-torsional (L-T) composite ultrasonic vibration [30]. One method uses two sets of longitudinally and tangentially polarized piezoelectric stacks to generate longitudinal and torsional vibrations respectively. However, this method is costly because tangentially polarized piezoelectric ceramic sheets are more expensive. In addition, it is difficult to maintain the frequency matching between the two resonances under different load conditions [31]. Another method creates straight grooves [32] and thread grooves [33] on the ultrasonic horn to convert longitudinal vibration into L-T composite ultrasonic vibration. However, the amplitude of the torsional vibration generated is very small for the reason that the horn is usually solid. In this paper, a hollow vibration converter with thread grooves is designed for LT-UAD purpose using a finite element model established in commercial FEM software. It is found that it can produce a higher torsional amplitude than using a solid converter, indicating that the designed vibration converter is more efficient.

This paper mainly focuses on a combination of theoretical analysis and experimental research, avoiding the uncertainty caused by the variability and complexity of the experimental environment in purely experimental research. Firstly, the kinematic analysis of LT-UAD is deeply studied. A condition for separating the tool from the workpiece is obtained and the net cutting time ratio in the LT-UAD process is studied. Furthermore, machining experiments of LT-UAD, UAD, and CD on Ti-6Al-4V alloy are carried out and the experimental results are consistent with the theoretical analysis. In addition, a regression model for flank wear width was established based on response surface methodology (RSM), and the variance analysis method is used to investigate the effect of machining parameters on tool wear and optimize the best processing conditions for LT-UAD of Ti-6Al-4V alloy. The application of statistical methods to deal with experimental data promotes the further development and innovation of similar methods in the field of machining.

2 Kinematic analysis of LT-UAD

2.1 Analysis of cutting trajectory

LT-UAD is a hybrid machining process in which two high-frequency and low-amplitude vibrations are superimposed on the rotational speed direction and the axial direction of the drilling bit respectively. Figure 1 delineates the basic motion model of LT-UAD, in which the motion is defined in a Cartesian coordinate system. The reverse direction of the feeding direction of the drilling bit represents the positive direction of Z-axis and the cutter rotates clockwise. In the LT-UAD processing, the drilling bit vibrates axially and

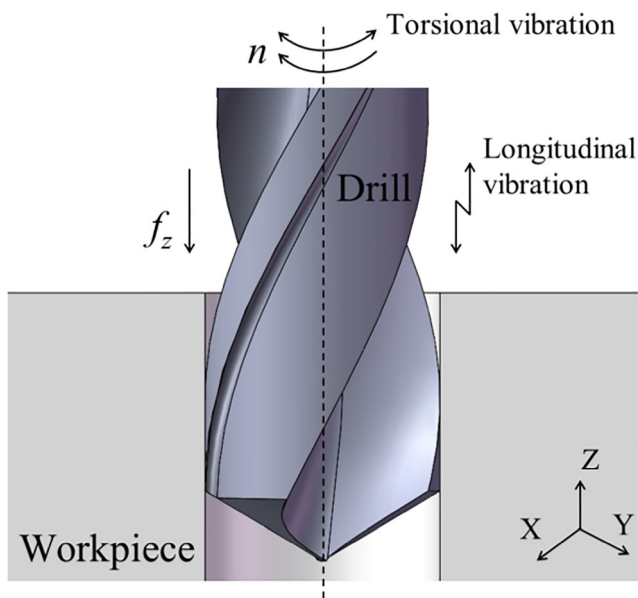


Fig. 1 Basic motion model of LT-UAD

circumferentially simultaneously at the same frequency and phase. The longitudinal vibration and torsional vibration of a point on the cutting edge can be expressed as:

$$\begin{cases} u_l(t) = A\sin(2\pi ft) \\ u_t(t) = \frac{B}{r_x} \cos(2\pi ft) \end{cases} \quad (1)$$

where A is the amplitude of longitudinal vibration; f is the frequency of ultrasonic vibration; r_x is the vertical distance from the point to the drill axis; B is the amplitude of torsional vibration amplitude, which is approximate as the arc length of rotation angle caused by torsional vibration. In the CD process, the trajectory of a point on the cutting edge can be described as follows [23]:

$$\begin{cases} x_c(t) = r_x \cos(2\pi nt) \\ y_c(t) = r_x \sin(2\pi nt) \\ z_c(t) = -f_z nt \end{cases} \quad (2)$$

where f_z is the feed rate and n represents the spindle speed. The motion equation of LT-UAD can be obtained by superimposing the two motions described in Eq. (1) and Eq. (2), which is delineated as follows:

$$\begin{cases} x_u(t) = r_x \cos \left[\frac{B}{r_x} \cos(2\pi ft) + 2\pi nt \right] \\ y_u(t) = r_x \sin \left[\frac{B}{r_x} \cos(2\pi ft) + 2\pi nt \right] \\ z_u(t) = -f_z nt + A\sin(2\pi ft) \end{cases} \quad (3)$$

The equation illuminates that the LT-UAD processing is mainly affected by machining parameters (spindle speed and feed rate) and ultrasonic vibration parameters (amplitude and

frequency). The longitudinal and tangential motions of drill bit are affected by longitudinal ultrasonic vibration and torsional ultrasonic vibration respectively. Under the given parameters, the trajectories of a point on the cutting edge during LT-UAD, L-UAD, and CD can be obtained, as shown in Fig. 2.

It can be seen that the trajectory in the CD process is a regular spiral, while that in the L-UAD process is approximately a sine curve distributed along the spiral. This phenomenon is attributed to the ultrasonic vibration in the vertical direction. Differently, the motion trajectory in the LT-UAD process presents a series of ellipses distributed along the spiral, because of the simultaneous presence of vibration in the longitudinal and tangential directions.

In order to more clearly describe the different trajectories of the three drilling methods, the trajectory in the three-dimensional (3D) space is displayed in a plane by expanding along the circumferential direction, as shown in Fig. 3. Obviously, longitudinal motion is the superposition of feed motion and axial vibration, while tangential motion is the superposition of rotary motion and torsional vibration. The motion equation can be expressed as follows:

$$\begin{cases} Z(t) = -f_z nt + A\sin(2\pi ft) \\ S(t) = 2\pi r_x nt + B\cos(2\pi ft) \end{cases} \quad (4)$$

where $Z(t)$ and $S(t)$ represent the longitudinal movement displacement and rotation arc length of drilling bit during LT-UAD, respectively. In the plane, the motion trajectory of a point on the cutting edge in the CD process is a straight line and that in L-UAD is a sine curve. In contrast, during LT-UAD, the ultrasonic vibration in the cutting direction and the feeding direction couples an elliptical motion track in the plane. This shows that LT-UAD is an intermittent cutting process of “feed-retract-feed,” in which the tool does not always contact with the workpiece.

2.2 Analysis of separation cutting characteristic in LT-UAD

According to the analysis of the movement trajectory of LT-UAD, the tool vibrates back and forth both in the feed

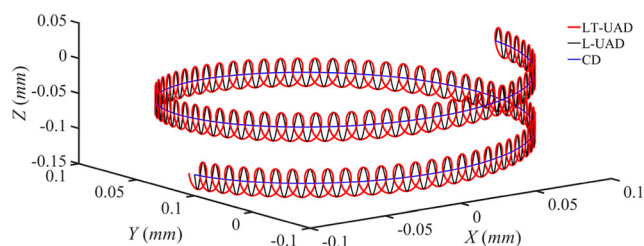


Fig. 2 3D trajectories of a point on the cutting edge during LT-UAD, L-UAD, and CD ($n = 18000$ r/min, $f_z = 0.08$ mm/r, $A = 20$ μ m, $B = 5$ μ m, $f = 20000$ Hz, and $r_x = 100$ μ m)

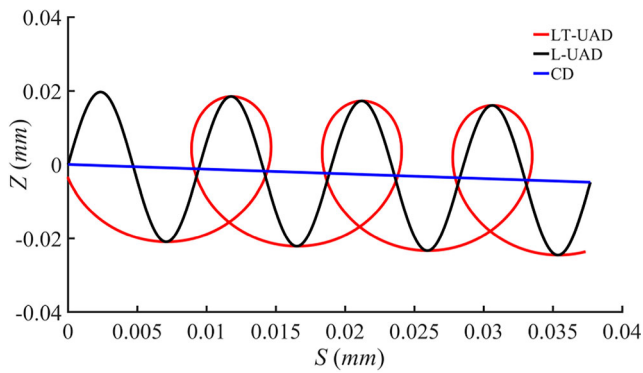


Fig. 3 2D trajectories of a point on the cutting edge during LT-UAD, L-UAD and CD process ($n = 18000$ r/min, $f_z = 0.08$ mm/r, $A = 20$ μ m, $B = 5$ μ m, $f = 20000$ Hz, and $r_x = 100$ μ m)

direction and the cutting direction in the process. As a result, the tool separates with the workpiece surface periodically. This is the separation cutting characteristic of LT-UAD. The intermittent separation is helpful to reduce cutting force and facilitate the dissipation of cutting heat, which is very beneficial to reduce tool wear and prolong the service life of the cutter.

However, the tool will not be separated from the workpiece when the inappropriate processing parameters are selected. Figure 4 shows the trajectory of the non-separated LT-UAD process. It can be seen from the figure that the tool enters the next cutting cycle before it could be separated from the workpiece. At this time, the tool is always in contact with the workpiece, which is the same as CD, and the advantage of LT-UAD in reducing tool wear will be weakened. Therefore, how to separate the tool from the workpiece is a topic worthy of in-depth study.

Figure 5 details the process of separation and contact between the tool and the workpiece, in which the cutting edge of the drill is discrete into countless tool units. The current cycle starts at t_1 and the tool starts to contact the workpiece at t_2 . The tool is at the maximum cutting depth at t_3 , and the speed component of the tool relative to the workpiece in the feed direction is 0. Then, the tool will move up and separate from the finished surface, but

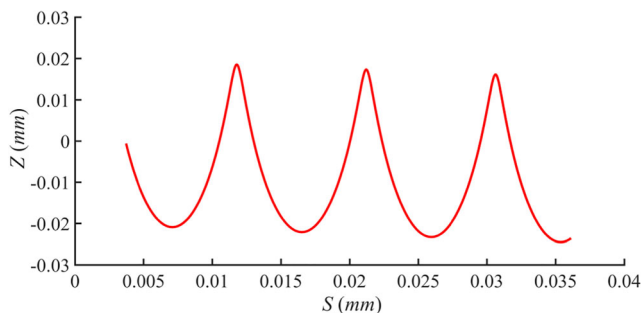


Fig. 4 Trajectories of the non-separated LT-UAD process ($n = 18000$ r/min, $f_z = 0.08$ mm/r, $A = 20$ μ m, $B = 0.8$ μ m, $f = 20000$ Hz, and $r_x = 100$ μ m)

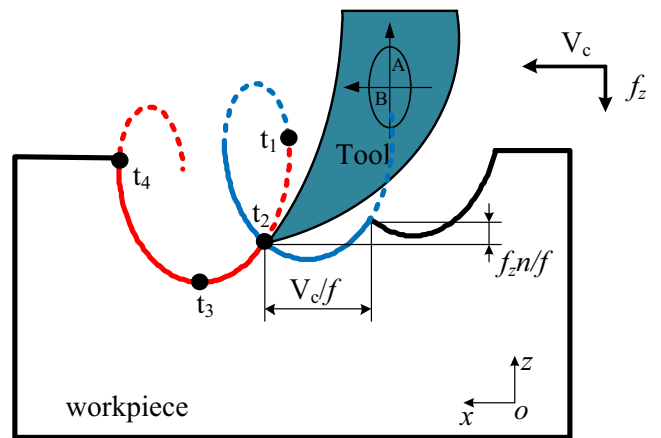


Fig. 5 Cutting diagram of LT-UAD

the rake face of the tool is still in contact with the workpiece at this time. At t_4 , the speed component of the tool relative to the workpiece in the cutting direction is 0, and then the tool will move backward and completely separate from the workpiece. Therefore, the condition for separating the tool from the workpiece can be expressed as follows:

$$\begin{cases} V_S = 2\pi r_x n - 2\pi f B \sin(2\pi f t) < 0 \\ V_Z = -f_z n + 2\pi f A \cos(2\pi f t) > 0 \end{cases} \quad (5)$$

where V_S and V_Z represent the speed component of the tool relative to the workpiece in the cutting direction and the speed component of the feed direction, respectively. Therefore, the following equation can be obtained:

$$\begin{cases} r_x n < f B \\ f_z n < 2\pi f A \end{cases} \quad (6)$$

Equation (6) reveals that when the vibration frequency is constant, whether the tool is separated from the workpiece in the LT-UAD process depends on the four processing parameters of the spindle speed, longitudinal amplitude, torsional amplitude, and feed rate. It was found that a lower feed rate, lower spindle speed and higher amplitude (both longitudinal and torsional) is more beneficial for separating the tool and the workpiece. The net cutting time ratio k is usually used to express the contact rate between the tool and the workpiece, which is defined as the ratio of the actual cutting time in a cycle to the vibration period. In theory, a lower value of k , which means that the contact time between tool and workpiece is less, is more helpful to reduce tool wear and prolong tool life. For the convenience of calculation, the net cutting time ratios in longitudinal and torsional directions (k_L and k_T) are derived, respectively, which can be expressed by Eq. (7) and Eq. (8), respectively.

$$f_z n(1 - k_L) = 2A f \sin(\pi k_T) \cos \left[\arccos \left(-\frac{f_z n}{2\pi A f} \right) - \pi k_T \right] \quad (7)$$

$$k_T = \frac{\arccos \left(-\frac{r m}{B f} \right) - \arcsin \left(\sqrt{1 - \left(\frac{r m}{B f} \right)^2} \right)}{\pi} \quad (8)$$

When the vibration frequency is constant, k_L is determined by feed rate, spindle speed, and longitudinal amplitude, while k_T is determined by spindle speed and torsional amplitude. In this study, the relationship between k_L , k_T , and processing parameters is investigated, as shown in Fig. 6. Both k_L and k_T increase with increasing spindle speed, which means that a high spindle speed is not conducive to the separation of the tool and the workpiece. Similarly, the value of k_L also tends to increase as the feed rate increases, indicating that a low feed rate should be used to reduce the contact rate between the tool and the workpiece, thereby reducing tool wear. It is also found that k_L and k_T decrease with increasing longitudinal amplitude and torsional amplitude, respectively. Even k_T reaches a maximum value of one when the torsional amplitude is sufficiently low, which means that the tool will not be separated from the workpiece, and it is not good for reducing tool wear. Therefore, it is recommended to choose as high amplitude as possible to obtain lower contact rate. In addition, k_L value is far less than 1 according

to the given parameter range, which shows that the tool is easier to separate from the machined surface of the workpiece in the feeding direction. This is due to the low feed rate and high vibration frequency usually adopted in the LT-UAD process.

3 Design of vibration converter

In this work, a vibration converter with spiral grooves is designed to generate L-T composite ultrasonic vibration in the front section of the tool and it is installed between the horn and the tool, as shown in Fig. 7. The input end and output end of the vibration converter are respectively connected with the horn and drill chuck by bolts. The working principle of the vibration converter is that when the longitudinal vibration is transmitted to the thread grooves, a tangential vibration component will be generated, thereby generating torsional vibration. In order to increase the tangential component and produce higher torsional amplitude, the vibration converter is designed as a hollow cylinder and the material is selected as 65Mn. In order to maximize the output amplitude, the design of the vibration converter is based on the half-wavelength theory; that is, the total length of the vibration converter and the tool is equal to half of the vibration wavelength. The design parameters of the vibration converter are listed in Table 1.

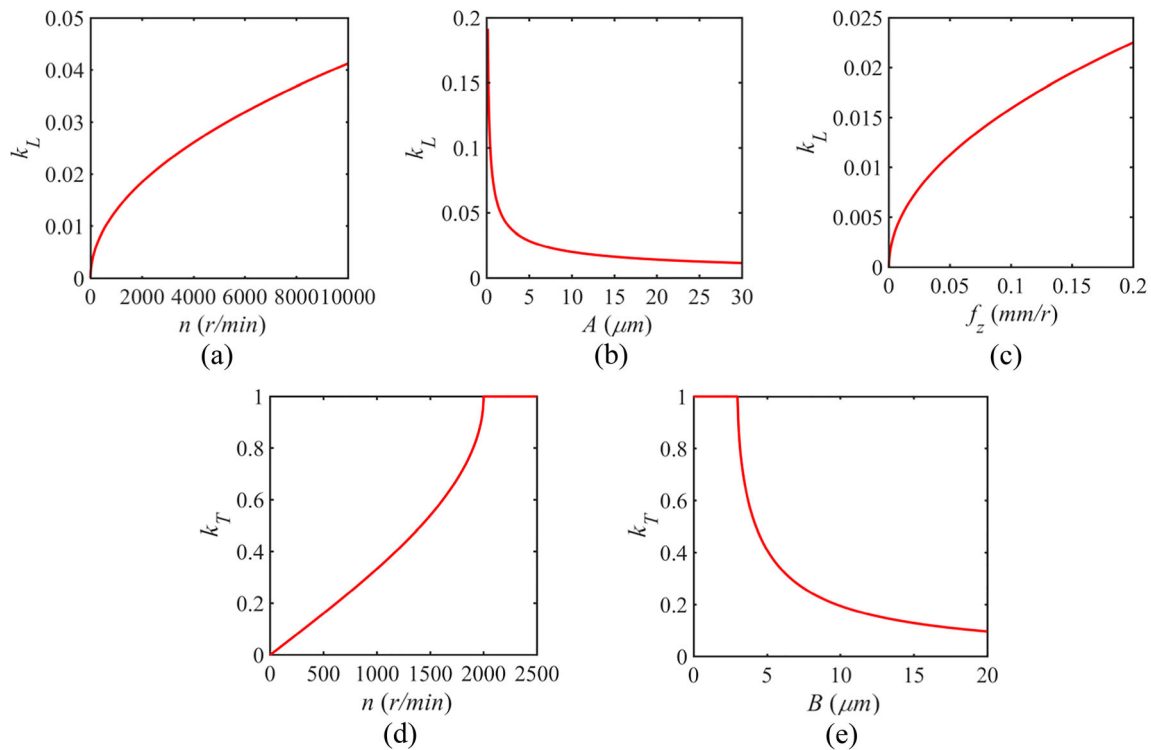


Fig. 6 Relationship between k_L , k_T , and processing parameters. **a** $f_z = 0.08$ mm/r, and $A = 20$ μm . **b** $f_z = 0.08$ mm/r, and $n = 1200$ r/min. **c** $A = 20$ μm , and $n = 1200$ r/min. **d** $f_z = 0.08$ mm/r, and $B = 5$ μm . **e** $f_z = 0.08$ mm/r, and $n = 1200$ r/min

Table 1 Design parameters of vibration converter

Design parameters	Values
Material	65Mn
Length, l (mm)	44
Outer diameter, D_1 (mm)	38
Inside diameter, D_2 (mm)	28
Direction of the spiral grooves	Left
Number of the spiral grooves	2
Pitch of the spiral grooves, P (mm)	15
Pitch of the spiral grooves, H (mm)	30
Width of the spiral grooves, a (mm)	2
Depth of the spiral grooves, h (mm)	5

Modal simulations of the proposed vibration converter were conducted in Abaqus software. The finite element model and modal analysis chart were illustrated in Fig. 8. It can be seen that a stable L-T composite vibration is produced at the output end of the converter. In addition, the resonance frequency of the vibration converter was 20.617 kHz, which approximated to the theoretical design requirements.

Undoubtedly, the amplitude of the output L-T composite vibration is directly related to the amplitude of the input longitudinal vibration for the designed vibration converter. Figure 9 shows the relationship between output amplitude and input amplitude, and the data in the figure comes from the dynamic simulation analysis of the vibration converter. In this work, the torsional amplitude component of the vibration converter is represented by the absolute average value of deformation displacement in X and Z directions at the output surface, which can be expressed as:

$$A_T = \frac{|A_x| + |A_z|}{2} \quad (9)$$

where A_x and A_z represent the deformation displacement in X direction and Z direction respectively. Obviously, the longitudinal vibration is greatly reduced when the ultrasonic vibration passes through the vibration converter. These could be

attributed to two reasons. First, a part of the energy is lost in the gap of spiral grooves in the process of ultrasonic vibration transmission. Second, the spiral grooves convert part of the longitudinal vibration into torsional vibration, which reduces the longitudinal amplitude. The ratio of amplitude of torsional vibration to longitudinal vibration m is often used to evaluate the efficiency of vibration converter. In this study, it can be expressed as:

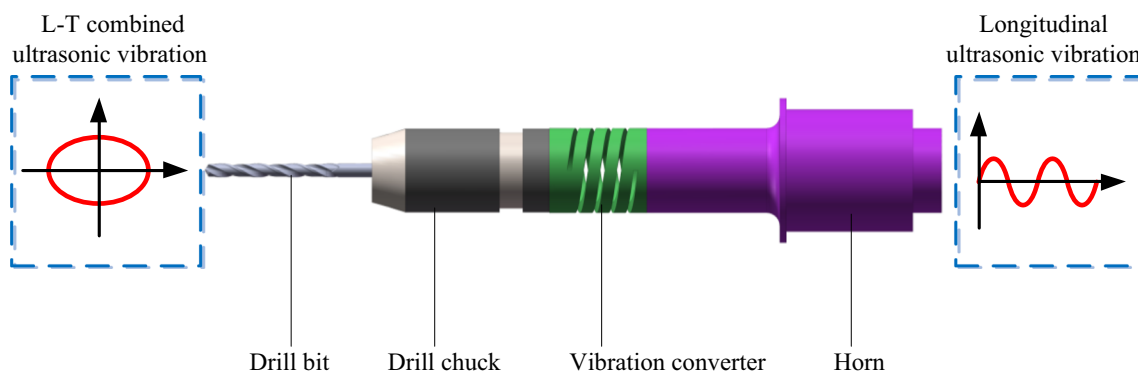
$$m = \frac{A_T}{A_L} \approx 1.5 \quad (10)$$

Compared with previous studies, the value of m is greater, which shows that the designed vibration converter can convert longitudinal vibration into L-T composite vibration more efficiently, and produce greater torsional vibration on the output surface.

4 Experimental details

4.1 Experimental setup and material

As shown in Fig. 10, the experiments were carried out on GSK 980TDB CNC lathe which has the advantages of high machining accuracy and high automation. More importantly, the processing parameters are wide in range and convenient to adjust. Usually, ultrasonic vibration is generated by an ultrasonic generator and an ultrasonic transducer. In this study, the 2000bdc-type ultrasonic generator manufactured by American Branson Ultrasonic Company was employed, and it can stably output an electric oscillation signal with a fixed frequency of 20 KHz. The ultrasonic transducer, made of piezoelectric ceramic plate with longitudinal polarization, converts this electric oscillation signal into mechanical vibration with the same frequency. Then, the mechanical vibration is amplified by the ultrasonic horn and transmitted to the input end of the vibration converter. As a key part, the vibration

**Fig. 7** Connecting format of vibration converter, horn, and drill chuck

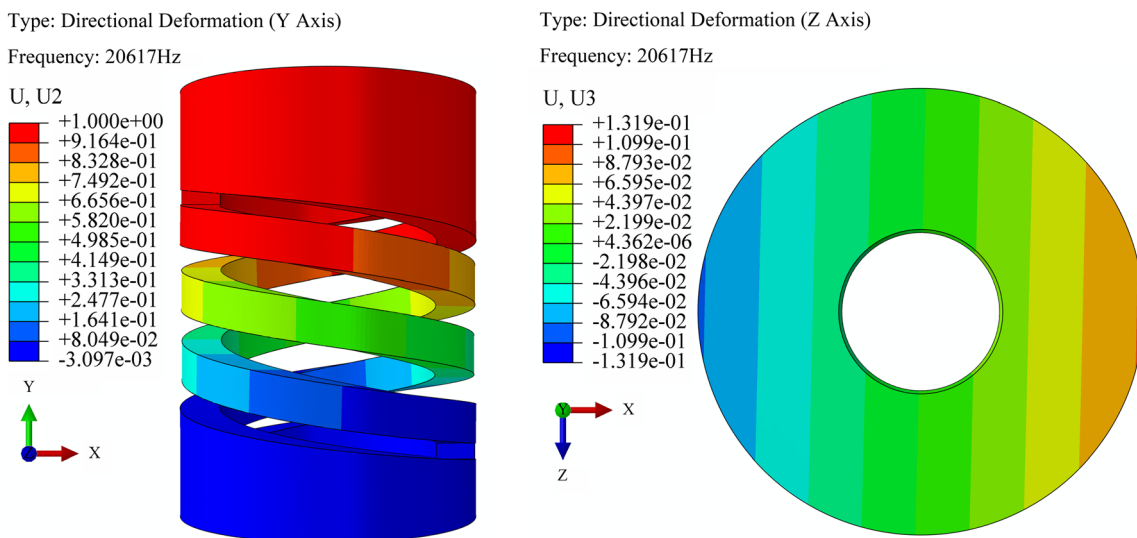


Fig. 8 Longitudinal component vibration and torsional component vibration of the grooved vibration converter

converter converts the longitudinal vibration into L-T composite ultrasonic vibration, so that LT-UAD can be realized. In this study, the actual amplitude on the tip of the drill bit was not measured because the ultrasonic generator can accurately control and display the amplitude.

In this work, drilling experiments were performed on Ti-6Al-4V alloy. The experimental materials were without heat treatment and the hardness is about 32 HRC. In the present work, cylindrical workpiece having the diameter of 20 mm and thickness of 10 mm were taken. Through-holes were drilled in dry condition. In view of the challenges of high cutting temperature and severe work hardening in titanium alloy processing, a tool with high hardness and high wear resistance is necessary. Carbide drills are the first choice, but it is easy to break in vibration drilling because of its low toughness. Finally, two-flute HSS-Co (M42) drills were used in this study and the specifications were given in Table 2.

4.2 Experimental measurement method

During the drilling process, the drill bit is in a semi-closed state and the heat dissipation conditions are relatively poor. As a result, the tool will inevitably wear out gradually. When the tool is worn, the machining accuracy of the workpiece is reduced, the cutting force and the cutting temperature are increased, and even the cutting cannot be continued. Therefore, tool wear directly affects machining efficiency, quality, and cost. Because of the convenience of measurement, the wear width VB on the tool flank is usually used as the standard for tool bluntness, as shown in Fig. 11. In this study, VB was measured using the VHX-1000E-type super depth 3D display system which has a 20–200 times zoom lens. Five different areas on the two flank surfaces of each drill bit were measured, and the average flank wear was calculated by taking the average of these five values to make sure the data is reasonable. The type of wear we focus on is abrasive wear.

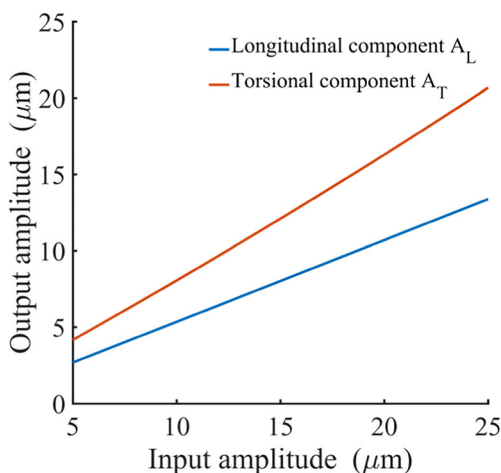


Fig. 9 Relationship between output amplitude and input amplitude

4.3 Design of experiments based on RSM

Comparative experiments were carried out first to study the effect of L-T composite ultrasonic vibration on tool wear. Then, the LT-UAD on Ti-6Al-4V alloy is further analyzed based on RSM to study the influences of different processing parameters on VB . RSM is a powerful statistical tool for mathematical modeling and optimization of processing parameters in scientific research [34] and it minimizes the number of experiments for a specific number of factors and their levels. In RSM, a second-order non-linear regression equation is used to model the relationship between the response variables, as shown in Eq. (11) [35].

$$S = a_0 + \sum_{i=1}^k a_i x_i + \sum_{i=1}^k a_{ii} x_i^2 + \sum_{i=1}^k a_{ij} x_i x_j \tag{11}$$

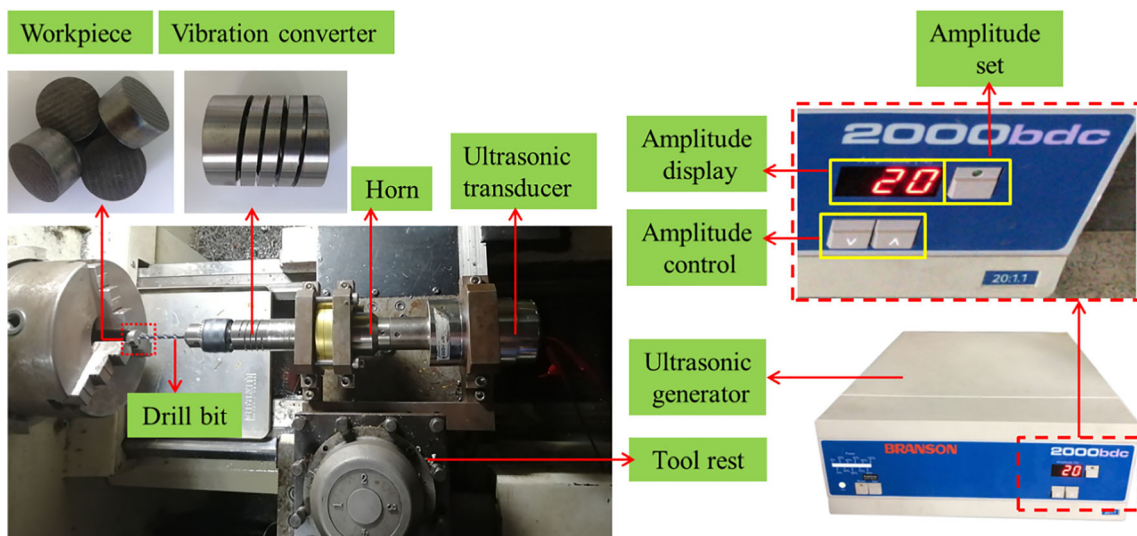


Fig. 10 Experimental setup

where S is the response; a_0 is the average of responses; a_i , a_{ii} , and a_{ij} are the coefficients of responses. The second, third, and fourth terms represent linear, higher order, and interaction effects respectively.

In this study, the longitudinal amplitude and torsional amplitude in LT-UAD are the longitudinal vibration component A_L and the torsional vibration component A_T outputted by the vibration converter, respectively. Since A_L and A_T cannot be controlled independently, the input amplitude of the vibration converter is selected as the control variable in the experiments. The input ultrasonic amplitude can be displayed and adjusted by controlling the front panel of the ultrasonic generator, as shown in Fig. 10. The ultrasonic vibration frequency is fixed at 20 kHz. In addition, the cutting parameters (spindle speed and feed rate) are controlled by the machine tool. Table 3 indicates the detailed processing parameters and their levels selected for the study.

5 Results and discussion

5.1 Effect of L-T composite ultrasonic vibration on tool wear

In order to compare the processing performance of LT-UAD, L-UAD, and CD, comparative experiments were

carried out, and the tool wear on the rake face and the flank face was measured. Figure 12 shows the wear on the rake face and flank face with the three different processing methods. In the figure, the drill bits are enlarged by 50 times, and in each trail, one hole was drilled on the workpiece with a new twist drill bit.

Obviously, whether it is on the rake face or the flank face, the drill bit in CD suffered the most severe wear, especially at the outermost edge of the drill bit. In the CD process, the tool always keeps in contact with the workpiece. As a result, the cutting heat generated in the cutting area is difficult to dissipate, and therefore, severe tool wear will occur. Especially, the cutting speed at the edge of the drill bit is the highest, which produces the most cutting heat, resulting in the most severe tool wear. Tool wear is greatly improved in L-UAD, but the wear at the edge of the drill bit is still obvious. In LT-UAD, the tool wear is minimal and uniform. The reason may be that the introduction of ultrasonic vibration makes the tool and the workpiece periodically separate and contact, which not only greatly reduces the friction between the tool and the workpiece, but also facilitates the emission of cutting heat. In addition, a torsional vibration component is generated on the drill bit, and the closer to the edge of the drill bit, the greater the vibration component. Therefore, it is easier for the drill bit to cut into the material, thereby reducing the wear at the edge of the tool.

Table 2 Specifications of drill bit

Diameter of drill	Material of drill	Overall length	Flute length	Point angle	Lip relief angle	Chisel edge angle	Helix angle
6 mm	HSS-Co (M42)	93 mm	58 mm	118°	10°	60°	30°

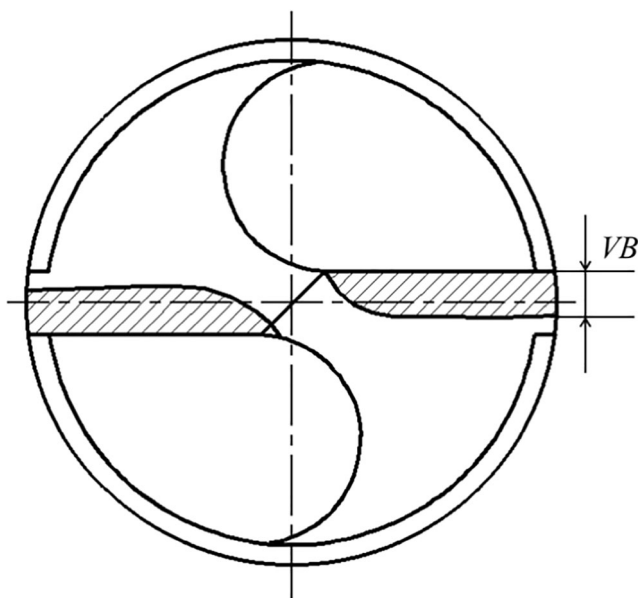


Fig. 11 Schematic diagram of flank wear width VB

Figure 13 shows the tool wear with the three processing methods after drilling three holes for each drill. The figure further indicates the inhibitory effect of L-T composite ultrasonic vibration on tool wear. In CD, very severe wear occurs on the flank face, and a large built-up edge is formed on the rake face, which is very unfavorable for material processing. Undoubtedly, this drill bit cannot be used any more. This situation is greatly improved when ultrasonic vibration is applied. Comparing Figs. 12 and 13, it can be found that the tool wear does not increase significantly in LT-UAD and L-UAD, although two more workpieces are processed. Therefore, it can be concluded that the introduction of ultrasonic vibration is beneficial to reduce tool wear, and 2D longitudinal torsional composite ultrasonic vibration is more advantageous than 1D longitudinal vibration. There is a high consistency between the experimental results and the theoretical analysis results, which indicates the rationality of the theoretical analysis and has important guiding significance for the subsequent experimental research.

Table 3 Detailed processing parameters and their levels

Experimental parameter	Symbol	Units	Levels				
			1	2	3	4	5
Amplitude	A	μm	10	12	16	20	23
Spindle speed	n	r/min	200	300	450	600	700
Feed rate	f_z	mm/r	0.02	0.04	0.06	0.08	0.10

5.2 Mathematical modeling and optimization of processing parameters

A standard RSM design called central composite design (CCD) comprising 20 runs is used for the experiments. It is very suitable for fitting a quadratic surface, which usually works well for mathematical modeling and optimization of machining parameters. Table 4 indicates the experimental design and the corresponding value of VB , which is used to establish the connection between the three control factors (amplitude, spindle speed, and feed rate) and response.

Equation (10) shows the second-order non-linear regression equation for flank wear width VB with linear, quadratic, and interactive terms, where the value of the regression coefficient is determined using Design Expert 8.0. The goodness of fit of the regression model is determined by the value of the R^2 coefficient, which provides a standard for evaluating how much variability in the observed response can be explained by the model. A higher R^2 value indicates that the model is more accurate. In this case, R^2 coefficient is found to be 0.9774, which shows that the regression model fits well with the experimental data.

$$\begin{aligned}
 VB = & 172.12356 - 0.58662n - 1580.97441f_z \\
 & + 5.59197A + 0.83458n \times f_z + 5.95625E-3n \\
 & \times A - 84.20313 f_z \times A + 5.21819E-4n^2 \quad (12)
 \end{aligned}$$

Table 5 represents the analysis of variance (ANOVA) for flank wear width VB , which further confirms the adequacy of the quadratic model (the Model Prob>F is less than 0.05). In addition, the results indicate that all the individual factors (amplitude, feed rate, and spindle speed) are significant for VB and the influences of the three factors in descending order are feed rate, amplitude, and spindle speed. The results also show the interactive effects of various factors on the response, indicating that the interaction term $f_z A$ is significant, while $n f_z$ and $n A$ are not significant. Figure 14 represents the influences of the processing parameters on VB . The value of VB tends to decrease considerably with an increase in amplitude, and a higher amplitude has a greater influence. The reason may be that a higher amplitude makes it easier for the tool to separate from the workpiece. This not only reduces the friction between the tool and the workpiece, but also makes it easier to dissipate the heat accumulated in the cutting area, thereby reducing tool wear.

Figure 14b indicates that the effect of feed rate and spindle speed on flank wear width is not linear. It is found that the flank wear width reaches the minimum at a feed rate of 0.046 mm/r when fixed ultrasonic amplitude at 16 μm and the spindle speed at 450 r/min. The flank wear width decreases with the increase of feed rate in the range of 0.02–0.046 mm/r. However, when the selected feed

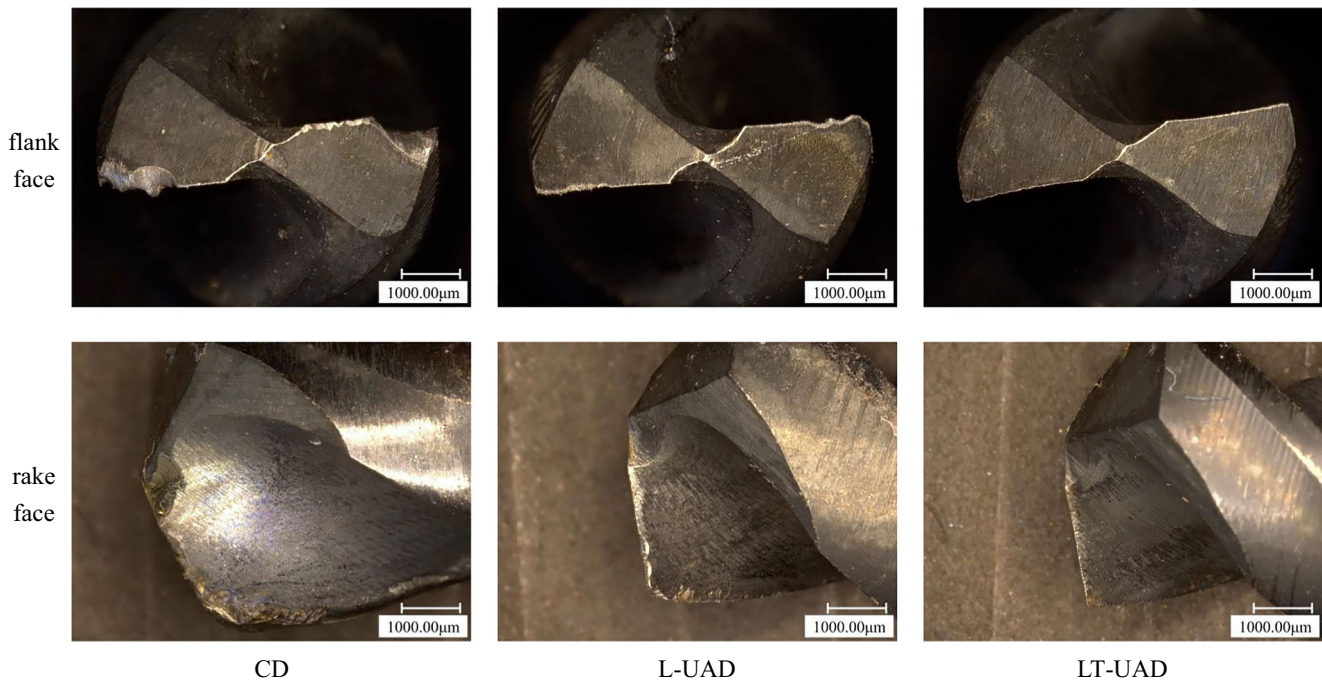


Fig. 12 Wear of the rake face and flank face in CD, L-UAD, and LT-UAD. ($n = 450$ r/min, $f_z = 0.06$ mm/r, $A = 16$ μ m, $f = 20000$ Hz, and $r = 3$ mm)

rate is greater than 0.046 mm/r, the flank wear width increases with the increase of the spindle speed. Through the previous theoretical analysis, it can be seen that the larger feed rate is not conducive to the separation of the tool and the workpiece. As a result, the contact time between the tool and the workpiece increases, which leads to increased tool wear. In addition, a higher feed rate

represents a larger cutting force and cutting temperature. There is no doubt that with the increase in cutting force and cutting temperature, the life of the drill is greatly reduced and tool wear increases. However, a too low feed rate will also increase tool wear. The reasons may be that the lower the feed rate, the more obvious the impact effect of the tool flank on the workpiece, which will increase

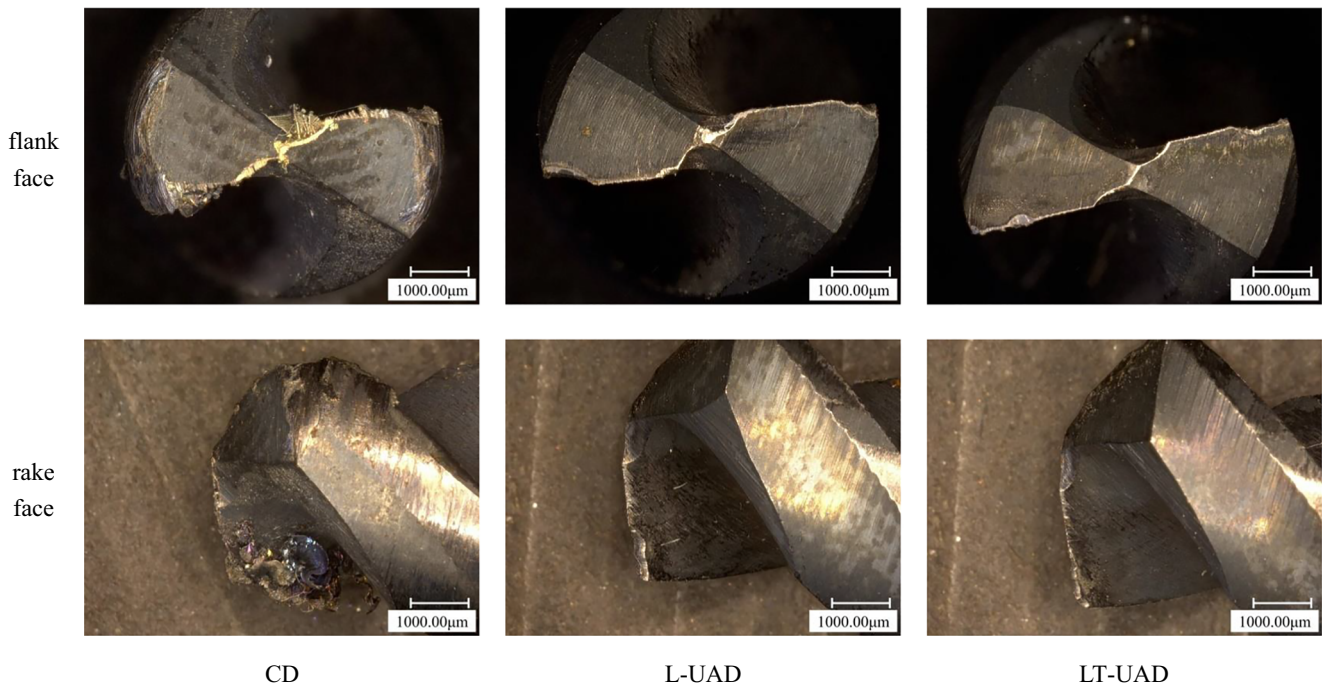


Fig. 13 Wear of the rake face and flank face in CD, L-UAD, and LT-UAD after each drill bit drills three workpieces ($n = 450$ r/min, $f_z = 0.06$ mm/r, $A = 16$ μ m, $f = 20000$ Hz, and $r = 3$ mm)

Table 4 Experimental design and the corresponding value of VB

Run	Parameters			VB (μm)
	Spindle speed n (r/min)	Feed rate f_z (mm/r)	Amplitude A (μm)	
1	450	0.06	16	39.03
2	450	0.06	16	40.12
3	450	0.03	16	41.04
4	450	0.06	16	39.25
5	600	0.08	12	81.72
6	300	0.04	20	37.31
7	450	0.06	16	39.45
8	200	0.06	16	63.22
9	450	0.06	16	40.84
10	700	0.06	16	83.02
11	450	0.06	16	40.96
12	300	0.04	12	54.25
13	450	0.06	10	29.34
14	450	0.06	23	10.25
15	450	0.09	16	102.06
16	600	0.08	20	52.13
17	300	0.08	20	28.31
18	600	0.04	12	73.76
19	300	0.08	12	53.16
20	600	0.04	20	40.15

tool wear. Therefore, it is necessary to select an appropriate feed rate to improve the tool durability in drilling Ti-6Al-4V alloy.

Spindle speed also has a significant effect on the drill wear. The flank wear width decreases with the increase of spindle speed in the range of 200–430 mm/r. And in the range of 430–700 mm/r, the flank wear width increases as the spindle speed increases. According to theoretical analysis, a higher speed makes it more difficult to separate the

tool from the workpiece, which will undoubtedly increase tool wear. Furthermore, higher friction is developed at a higher spindle speed, and that is main cause for generation of heat in the cutting area. The heat collected in the cutting area increases wear on the flank. It was also noted that excessively low will also lead to greater tool wear. This is mainly because an excessively low spindle speed will make it difficult for cutting deformation, thereby increasing tool wear.

Table 5 ANOVA results for VB

Source	Sum of squares	DOF	Mean square	F value	p value	Prob > F
Model	10016.05	9	1112.89	48.04	< 0.0001	Significant
n -Spindle speed	245.86	1	245.86	10.61	0.0086	Significant
f_z -Feed rate	3001.81	1	3001.81	129.58	< 0.0001	Significant
A -Amplitude	2246.89	1	2246.89	96.99	< 0.0001	Significant
nf_z	50.15	1	50.15	2.16	0.1720	
nA	102.17	1	102.17	4.41	0.0621	
f_zA	363.02	1	363.02	15.67	0.0027	Significant
n^2	1936.03	1	1936.03	83.57	< 0.0001	Significant
f_z^2	1743.31	1	1743.31	75.25	< 0.0001	Significant
A^2	139.04	1	139.04	6.00	0.0343	Significant
Residual	231.67	10	23.17			
Total	10247.72	19				

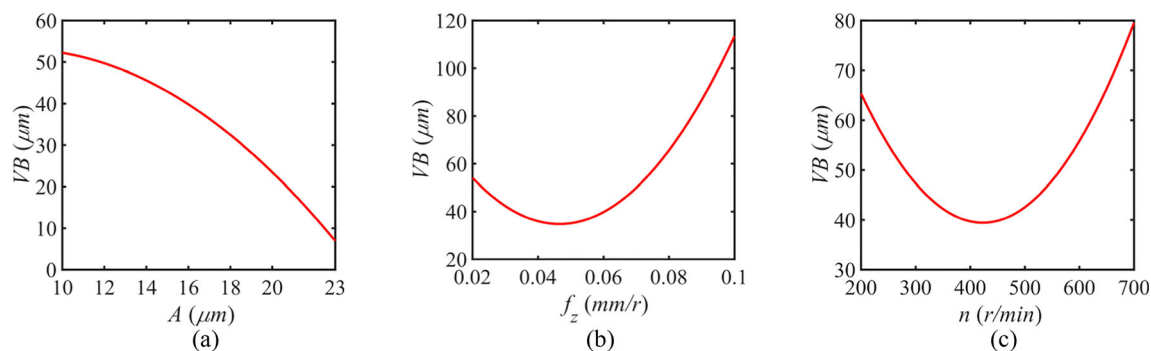


Fig. 14 Influence of the processing parameters (amplitude, feed rate, and spindle speed) on VB . **a** $n = 450$ r/min, and $f_z = 0.06$ mm/r. **b** $n = 450$ r/min, and $A = 16$ μm . **c** $f_z = 0.06$ mm/r, and $A = 16$ μm

In this study, Design-Expert software is used to optimize the machining parameters with the goal of minimizing the flank wear width VB , and the variation ranges of amplitude, feed rate, and spindle speed are 0–23 μm , 0.02–0.10 mm/r, and 200–700 r/min, respectively. Verification experiments are conducted with the recommended sources, and the test results are shown in Table 6. Because the influence of amplitude on VB value is linear, and the minimum VB value obtained when the amplitude is maximum, the amplitude is kept constant at 23 μm in the table. Obviously, the minimum VB value is obtained by using the machining parameters of run 1. Therefore, the optimum levels of machining parameters are obtained as 23 μm of amplitude, 0.06 mm/r of feed rate, and 385 r/min of spindle speed. The experimental results also indicate that the established prediction model of VB is reliable in view of the small error between the predicted value and the actual value. The error may be caused by machine tool flutter and measurement. The error decreases with the increase of spindle speed and the decrease of feed rate, which may be due to the better rotational stability and smaller flutter of the machine tool with a high spindle speed and a lower feed rate.

6 Conclusions

This paper focuses on theoretical analysis and experimental research of tool wear in LT-UAD on Ti-6Al-4V alloy. Some

important and meaningful conclusions are summarized as follows:

- (1) In the LT-UAD process, there is periodic separation and contact between the tool and the workpiece, which is beneficial to reducing tool wear. A condition for the separation of the tool and the workpiece was found, indicating that a lower feed rate, a lower spindle speed, and a higher amplitude are more conducive to separating the tool and the workpiece.
- (2) Both theoretical analysis and experimental results indicate that the introduction of ultrasonic vibration is beneficial to reducing tool wear, and 2D longitudinal-torsional composite ultrasonic vibration is more advantageous than 1D longitudinal vibration.
- (3) In the LT-UAD of Ti-6Al-4V alloy, all the factors (feed rate, spindle speed, and amplitude) have a significant effect on the flank molding width VB . The feed rate is most significant for VB followed sequentially by the amplitude and spindle speed. Furthermore, VB value decreases as the amplitude increases. However, the effect of feed rate and spindle speed on VB is not linear, and a spindle speed and feed rate that is too high or too low will cause greater tool wear.
- (4) A regression model for VB is established based on the response surface method. The results of ANOVA indicate that this model is effective and reliable, and the VB value under different

Table 6 Experimental results

Run	Amplitude (μm)	Spindle speed (r/min)	Feed rate (mm/r)	Predicted VB	Actual VB	%Differences
1	23	385	0.06	4.50	4.79	− 6.05%
2	23	358	0.06	5.39	5.05	6.73%
3	23	315	0.06	7.17	7.88	− 9.01%
4	23	375	0.05	5.49	5.89	− 7.28%
5	23	439	0.05	6.25	6.72	− 6.99%
6	23	461	0.05	8.05	7.73	4.14%

processing parameters can be accurately predicted with this model.

- (5) The optimum levels of machining parameters are obtained as the amplitude of 23 μm , the feed rate of 0.06 mm/r, and the spindle speed of 385 r/min. The results of the verification experiment show that minimum tool wear is indeed obtained with the optimized machining parameters. The error between the predicted value and the actual value is only -6.05% , which shows that this prediction model is reliable and accurate.

Funding The authors are grateful for the financial support received from the National Natural Science Foundation of China (Grant No. 51875097).

Availability of data and materials All data used in the manuscript are available as submitted.

Code availability Not applicable.

Declarations

Ethical approval Not applicable.

Consent to participate Not applicable.

Consent to publish Not applicable.

Competing interests The Authors wish to declare that there are no known competing interests related to this publication.

References

- Ma J, Andrus P, Condoor S, Lei S (2015) Numerical investigation of effects of cutting conditions and cooling schemes on tool performance in up milling of Ti-6Al-4V alloy. *Int J Adv Manuf Technol* 78(1-4):361–383
- Manjaiah M, Narendranath S, Basavarajappa S (2014) A review on machining of titanium based alloys using EDM and WEDM. *Rev Adv Mater Sci* 36(2):89–111
- de Lacalle LNL, Rivero A, Lamikiz A (2009) Mechanistic model for drills with double point-angle edges. *Int J Adv Manuf Technol* 40(5-6):447–457
- Parida AK (2018) Simulation and experimental investigation of drilling of Ti-6Al-4V alloy. *Int J Lightweight Mater Manuf* 1(3):197–205
- Yi S, Li G, Ding S, Mo J (2017) Performance and mechanisms of graphene oxide suspended cutting fluid in the drilling of titanium alloy Ti-6Al-4V. *J Manuf Process* 182–193
- Trivedi DB, Kumar A, Joshi SS (2018) Surface integrity analysis in heat sink-based dry drilling of titanium alloy. *Mater Today Proc* 5(9):19529–19538
- Trivedi DB, Kumar A, Joshi SS (2018) Drilling of titanium alloy using heat sink-based ice water cooling. *Procedia Manuf* 26:633–644
- Rodríguez-Barrero S, Fernández-Larriñoa J, Azkona I et al (2014) Enhanced performance of nanostructured coatings for drilling by droplet elimination. *Mater Manuf Process* 31(5):593–602
- Chatterjee S, Mahapatra SS, Abhishek K (2016) Simulation and optimization of machining parameters in drilling of titanium alloys. *Simul Model Pract Theory* 62:31–48
- Muhamad Nasir M, Safian S (2014) Effect of drill point angle on surface integrity when drilling titanium alloy. *Adv Mater Res* 845:966–970
- Yang H, Ding W, Chen Y, Laporte S, Xu J, Fu Y (2019) Drilling force model for forced low frequency vibration assisted drilling of Ti-6Al-4V titanium alloy. *Int J Mach Tool Manu* 146:103438
- Suárez A, Veiga F, de Lacalle LNL, Polvorosa R, Lutze S, Wretland A (2016) Effects of ultrasonics-assisted face milling on surface integrity and fatigue life of Ni-Alloy 718. *J Mater Eng Perform* 25(11):5076–5086
- Xu Y, Gao F, Zou P, Zhang Q, Fan F (2020) Theoretical and experimental investigations of surface roughness, surface topography, and chip shape in ultrasonic vibration-assisted turning of Inconel 718. *J Mech Sci Technol* 34(9):3791–3806
- Tian Y, Zou P, Yang X, Kang D (2020) Study on chip morphology and surface roughness in ultrasonically assisted drilling of 304 stainless steel. *Int J Adv Manuf Technol* 108:2079–2090
- Xu Y, Wan Z, Zou P, Huang W, Zhang G (2020) Experimental study on cutting force in ultrasonic vibration-assisted turning of 304 austenitic stainless steel. *P i Mech Eng B J Eng* 0954405420957127
- Zhang DY, Feng XJ, Wang LJ, Chen DC (1994) Study on the drill skidding motion in ultrasonic vibration microdrilling. *Int J Mach Tool Manu* 34(6):847–857
- Zhang LB, Wang LJ, Liu XY, Zhao HW, Wang X, Luo HY (2001) Mechanical model for predicting thrust and torque in vibration drilling fibre-reinforced composite materials. *Int J Mach Tool Manu* 41(5):641–657
- Azarhoushang B, Akbari J (2007) Ultrasonic-assisted drilling of Inconel 738-lc. *Int J Mach Tool Manu* 47(7):1027–1033
- Barani A, Amiri S, Paktinat H, Fadaei Tehrani A (2014) Built-up edge investigation in vibration drilling of al2024-t6. *Ultrasonics* 54(5):1300–1310
- Baghlani V, Mehbudi P, Akbari J, Nezhad EZ, Sarhan AAD, Hamouda AMS (2016) An optimization technique on ultrasonic and cutting parameters for drilling and deep drilling of nickel-based high-strength Inconel 738lc superalloy with deeper and higher hole quality. *Int J Adv Manuf Technol* 82(5-8):877–888
- Lotfi M, Amiri S (2017) Experimental and numerical study of ultrasonically-assisted drilling. *Ultrasonics* 75:185–193
- Liang W, Xu J, Ren W, Liu Q, Yu H (2019) Study on the influence of tool point angle on ultrasonic vibration-assisted drilling of titanium alloy. *Int J Adv Manuf Technol* 1–14
- Chen S, Zou P, Tian Y, Duan J, Wang W (2019) Study on modal analysis and chip breaking mechanism of Inconel 718 by ultrasonic vibration-assisted drilling. *Int J Adv Manuf Technol* 105(1-4):177–191
- Chen S, Zou P, Wu H, Kang D, Wang W (2019) Mechanism of chip formation in ultrasonic vibration drilling and experimental research. *P i Mech Eng C-J Mec* 233(15):5214–5226
- Celaya A, Lacalle LNL, Campa FJ, Lamikiz A (2010) Ultrasonic assisted turning of mild steels. *Int J Mater Prod Technol* 37(1-2):60–70
- Haidong ZHAO, Shuguang L, Ping ZOU, Di K (2017) Process modeling study of the ultrasonic elliptical vibration cutting of Inconel 718. *Int J Adv Manuf Technol* 92(5-8):2055–2068
- Haidong Z, Ping Z, Wenbin M, Zhongming Z (2016) A study on ultrasonic elliptical vibration cutting of Inconel 718. *Shock Vib* 2016:1–11
- Liu J, Jiang X, Han X, Zhang D (2019) Influence of parameter matching on performance of high-speed rotary ultrasonic elliptical vibration-assisted machining for side milling of titanium alloys. *Int J Adv Manuf Technol* 101(5-8):1333–1348

29. Liu J, Jiang X, Han X, Gao Z, Zhang D (2019) Effects of rotary ultrasonic elliptical machining for side milling on the surface integrity of Ti-6Al-4V. *Int J Adv Manuf Technol* 101(5-8):1451–1465
30. Liu S, Shan X, Cao W, Yang Y, Xie T (2017) A longitudinal-torsional composite ultrasonic vibrator with thread grooves. *Ceram Int* 43:S214–S220
31. Qi A, Friend J, Yeo L (2007) An analytical model for a twisted beam piezoelectric ultrasonic micromotor. 5th Australasian Congress on Applied Mechanics 325–330
32. Yang C, Shan X, Xie T (2015) A new piezoelectric ceramic longitudinal-torsional composite ultrasonic vibrator for wire drawing. *Ceram Int* 41:S625–S630
33. Al-Budairi H, Lucas M, Harkness P (2013) A design approach for longitudinal-torsional ultrasonic transducers. *Sensor Actuators A Phys* 198:99–106
34. Thakre AA, Soni S (2016) Modeling of burr size in drilling of aluminum silicon carbide composites using response surface methodology. *Eng Sci Technol* 19(3):1199–1205
35. Chelladurai SJS, Murugan K, Ray AP, Upadhyaya M, Narasimharaj V, Gnanasekaran S (2020) Optimization of process parameters using response surface methodology: a review. *Materials Today: Proceedings*. <https://doi.org/10.1016/j.matpr.2020.06.466>

Publisher's note Springer Nature remains neutral with regard to jurisdictional claims in published maps and institutional affiliations.